coatings

MDPI

Article

Corrosion Inhibition Properties of Waterborne Polyurethane/Cerium Nitrate Coatings on Mild Steel

Mohammad Mizanur Rahman [1,*], Md. Hasan Zahir [2], Md. Bashirul Haq [3,*], Dhafer A. Al Shehri [3] and A. Madhan Kumar [1]

1 Center of Research Excellence in Corrosion, King Fahd University of Petroleum and Minerals, Dhahran 31261, Saudi Arabia; madhankumar@kfupm.edu.sa
2 Center of Research Excellence in Renewable Energy, King Fahd University of Petroleum and Minerals, Dhahran 31261, Saudi Arabia; hzahir@kfupm.edu.sa
3 Department of Petroleum Engineering, College of Petroleum and Geosciences, King Fahd University of Petroleum and Minerals, Dhahran 31261, Saudi Arabia; alshehrida@kfupm.edu.sa
* Correspondence: mrahman@kfupm.edu.sa (M.M.R.); bhaq@kfupm.edu.sa (M.B.H.); Tel.: +966-13-860-7210 (M.M.R.)

Received: 26 September 2017; Accepted: 10 January 2018; Published: 15 January 2018

Abstract: Waterborne polyurethane (WBPU)/cerium nitrate ($Ce(NO_3)_3$) dispersions were synthesized with different defined $Ce(NO_3)_3$ content. All pristine dispersions were stable with different poly(tetramethylene oxide) glycol (PTMG) number average molecular weights (Mn) of 650, 1000, and 2000. The interaction between the carboxyl acid salt group and $Ce(NO_3)_3$ was analyzed by Fourier-transform infrared spectroscopy (FT-IR) and X-ray photoelectron spectroscopy (XPS) techniques. Coating hydrophilicity, water swelling (%), water contact angle, leaching, and corrosion protection efficiency were all affected when using different $Ce(NO_3)_3$ content and PTMG molecular weights. The maximal corrosion protection of the WBPU coating was recorded using a higher molecular weight of PTMG with 0.016 mole $Ce(NO_3)_3$ content.

Keywords: waterborne polyurethane; corrosion; cerium nitrate; coating

1. Introduction

Highly toxic inhibitors and solvents are being phased out and replaced by benign alternatives in coating industries [1,2]. In the last decade, it was established that volatile organic compounds (VOCs) and toxic inhibitors must be controlled to the lowest possible levels. The harmful impact of VOC coatings has led to the substitution of solvent-borne systems with waterborne systems [3]. Among the recently developed systems, polyurethane (PU) exhibits a special value over other waterborne coatings. Therefore, PU coatings are widely used in many industrial applications [4–7].

Using environmentally friendly polyurethane (PU) (e.g., waterborne polyurethane, WBPU) coatings for corrosion protection has garnered attention over the past couple of years, as certain pioneering researchers have improved the PU coating for barrier and scratch resistance [8–11]. PU is mainly composed of polyol (called the soft segment) and diisocyanate (called the hard segment). The polyol contributes to the elastomeric properties, and the diisocyanate controls the coating's mechanical properties. There are different types of polyols, such as polyether polyol, polyester polyol, silanol, etc. PU coating properties can be altered by tuning polyols and their contents [4,5]. In the last decade, PU technology has emerged as an attractive approach for developing next-generation PU coatings for broader industrial applications [4,5,11]. PU coatings are promising in antifouling, anticorrosion, antibacterial, anti-scratching and self-healing coatings [4,5,7]. Different anticorrosion coatings have been prepared by using different monomers, nanoparticles, and inhibitors [4,5].

Researchers have demonstrated that inhibitors are excellent corrosion protectors when used properly in coatings; however, their effectiveness also depends on the overall synthesis criteria, the interaction between the doped inhibitor and coating matrices, as well as the final deposited coating (thickness, adhesion, hydrophobicity, etc.) on the substrates [12–14]. Inhibitor solubility is another important criterion when using inhibitors in coatings. Usually, freely water-soluble inhibitors are less attractive than non-water-soluble inhibitors, since the former have a chance in the coating industry as those inhibitors have a chance of being easily leached, which decreases the life time of the dried coatings. However, the water-soluble inhibitors can be mixed easily with environmentally friendly water-based coatings. Therefore, water-soluble inhibitors might prove useful when the inhibitor can be retained in the coating for a longer time.

Different cerium salts (e.g., cerium phosphates, cerium cinnamates, and cerium silicates) exhibit good corrosion protection [15–17]. In some cases, water-soluble cerium salts such as cerium nitrate, $Ce(NO_3)_3$, and cerium chloride, $CeCl_3$, have also been used as inhibitors for the corrosion process [18]. In most of these cases, these inhibitors have been used in organic solvent-based coatings. It is difficult to find any reports on using cerium nitrate ($Ce(NO_3)_3$, a water-soluble inhibitor) in waterborne polyurethane (WBPU) coatings. In this study, three series of WBPU/$Ce(NO_3)_3$ dispersions were prepared with defined $Ce(NO_3)_3$ content using three different molecular weights of poly(tetramethylene oxide) glycol (PTMG) (M_n = 650, 1000, and 2000). The interaction of $Ce(NO_3)_3$ with PU was analyzed by Fourier-transform infrared spectroscopy (FT-IR) and X-ray photoelectron spectroscopy (XPS) analysis. The stability of the cerium salt dispersion was checked visually. The substrate for the coating was mild steel, and the synthesized WBPU/$Ce(NO_3)_3$ dispersions were used as a coating material. Corrosion testing was undertaken by potentiodynamic polarization (PDP) analysis. In addition, a leaching test at defined intervals was conducted to investigate the effect of $Ce(NO_3)_3$ content and PTMG molecular weight on the leaching of cerium salt.

2. Materials and Methods

Poly(tetramethylene oxide) glycol (PTMG, M_n = 650, 1000, 2000, Sigma Aldrich, St. Louis, MO, USA) samples were vacuum dried at 90 °C for three hours prior to use. Triethylamine (TEA, Sigma Aldrich), *N*-methyl-2-pyrrolidone (NMP, Sigma Aldrich), 4,4-dicyclohexylmethane diisocyanate (H_{12}MDI, Sigma Aldrich), and ethylene diamine (EDA, Sigma Aldrich) were used after dehydration with 4 Å molecular sieves for seven days. Dimethylolpropionic acid (DMPA, Sigma Aldrich), $Ce(NO_3)_3$ (Sigma Aldrich), and dibutyltindilaurate (DBTDL, Sigma Aldrich) were used as received.

2.1. Pristine Waterborne Polyurethane (WBPU) Dispersion Preparation

Pristine WBPU dispersion was prepared based on our previous report [7]. The solid content of the WBPU dispersion was fixed at 30 wt %. During preparation, the pre-polymer (NCO-terminated) was obtained by charging DMPA, H_{12}MDI, and PTMG. A very small amount of DBTDL was added during the reaction of PTMG and H_{12}MDI. 10 wt % methyl ethylketone (MEK) was added to the pre-polymer to lower the viscosity of pre-polymer. To neutralize the carboxyl group of DMPA, TEA was added to the pre-polymer mixture. Distilled water was added to the neutralized pre-polymer, which was followed by chain extension by adding EDA. Finally, MEK was evaporated from the WBPU dispersion.

2.2. Preparation of WBPU/Ce(NO$_3$)$_3$ Dispersion

A physical intermixing technique was applied to prepare the WBPU/$Ce(NO_3)_3$ dispersions. An exact amount (see Table 1) of $Ce(NO_3)_3$ was mixed with water to make a clear solution, which was mixed at the dispersion step of WBPU. The solid content was also fixed at 30 wt %.

Table 1. Sample designation, composition, and stability of dispersions. DMPA: dimethylolpropionic acid; EDA: ethylene diamine; H_{12}MDI: 4,4-dicyclohexylmethane diisocyanate; PTMG: poly(tetramethylene oxide) glycol; TEA: trimethylamine; WBPU: waterborne polyurethane.

Sample Designation	Composition (Mole)					PTMG (wt %)	$Ce(NO_3)_3$ (Mole)	Stability
	PTMG	DMPA	H_{12}MDI	TEA	EDA			
WBPU-650	0.525	0.760	1.83	0.760	0.550	32	0	Stable
WBPU-650-Ce-4	0.525	0.760	1.83	0.760	0.550	32	0.004	Stable
WBPU-650-Ce-8	0.525	0.760	1.83	0.760	0.550	32	0.008	Stable
WBPU-650-Ce-12	0.525	0.760	1.83	0.760	0.550	32	0.012	Unstable
WBPU-650-Ce-16	0.525	0.760	1.83	0.760	0.550	32	0.016	Unstable
WBPU-1000	0.525	0.760	1.83	0.760	0.550	43	0	Stable
WBPU-1000-Ce-4	0.525	0.760	1.83	0.760	0.550	43	0.004	Stable
WBPU-1000-Ce-8	0.525	0.760	1.83	0.760	0.550	43	0.008	Stable
WBPU-1000-Ce-12	0.525	0.760	1.83	0.760	0.550	43	0.012	Stable
WBPU-1000-Ce-16	0.525	0.760	1.83	0.760	0.550	43	0.016	Unstable
WBPU-2000	0.525	0.760	1.83	0.760	0.550	60	0	Stable
WBPU-2000-Ce-4	0.525	0.760	1.83	0.760	0.550	60	0.004	Stable
WBPU-2000-Ce-8	0.525	0.760	1.83	0.760	0.550	60	0.008	Stable
WBPU-2000-Ce-12	0.525	0.760	1.83	0.760	0.550	60	0.012	Stable
WBPU-2000-Ce-16	0.525	0.760	1.83	0.760	0.550	60	0.016	Stable
WBPU-2000-Ce-20	0.525	0.760	1.83	0.760	0.550	60	0.020	Unstable

The solid content of all samples was 30 wt %.

2.3. Coating onto Mild Steel Substrate

The synthesized coating solution was coated onto the mild steel through the autocoater. The wet coating thickness was 100 µm. All coatings dried at room temperature, and then oven dried at 70 °C for 24 h to remove the solvent perfectly.

2.4. Characterization

FT-IR spectroscopy (Impact 400D, Nicolet, Madison, WI, USA) was used to characterize the PU polymer.

The zeta potential value of the dispersion was analyzed by a Malvern Zetasizer 3000, zeta-potential analyzer (Malvern Instruments, Malvern, UK). During analysis, the temperature was fixed at 25 °C.

X-ray photoelectron spectroscopy (XPS) (ESCA 250 XPS, Thermo Scientific, East Grinstead, UK) was used to analyze the polymer surface.

For the swelling study, all films were immersed in water for 48 h at 30 °C and the swelling (%) was determined from the weight increase as [7]:

$$\text{Swelling (\%)} = (W - W_0/W_0) \times 100 \quad (1)$$

where W_0 is the weight of the dried film and W is the weight of the film at equilibrium swelling.

A Theta Optical tensiometer (Attension, Biolin Scientific, Helsinki, Finland) was used to analyze the water contact angle of the coatings.

The leaching rate was analyzed by UV (UV2600 UV-Vis spectrometer, Shimadzu, Kyoto, Japan) analysis, following a previous report [19]. The coated sample was immersed in water and slowly vibrated. After a certain time, the water was collected for UV analysis. From the spectra, the concentration of dissolved cerium ions was calculated.

A GAMRY3000 corrosion measurement system was used for potentiodynamic polarization (PDP) analysis, according to our previous report [20]. The reference electrode was −2 V vs. Ref. In this study, the electrochemical cell consisted of a prepared coated electrode as a working electrode, a graphite rod as a counter electrode, a saturated calomel electrode (SCE) as a reference electrode, and 3.5 wt % sodium chloride (NaCl) as the electrolyte. A surface Mask (GAMRY) of 1 cm^2 was used to mask the analyzed surface.

Potentiodynamic polarization plots were attained at the potential in the Tafel region with ±250 mV from open circuit potential (OCP) at a scan rate of 1 mV·s^{-1}. The corrosion rate (CR) of the coated samples was calculated from Tafel polarization curves using the following equation:

$$CR = 3268 \times i_{corr} \times EW/D \quad (2)$$

where i_{corr} represents the corrosion current density (mA·cm^{-2}), EW is the equivalent weight of the sample, and D is the density (g·cm^{-3}) of the sample. Further, the polarization resistance (R_p) was calculated using the following Stern–Geary equation:

$$R_p = \beta_a \times \beta_c / 2.303\ (i_{corr})\ (\beta_a + \beta_c) \quad (3)$$

where β_a and β_c represent the anodic and cathodic slopes, respectively. In addition, the inhibition efficiency (η) of coatings with and without the addition of $Ce(NO_3)_2$ were also calculated using the following relation:

$$\eta(\%) = R_p(\text{inhibit}) - R_p(\text{uninhibit})/R_p(\text{inhibit}) \times 100 \quad (4)$$

where R_p(inhibit) and R_p(uninhibit) represent the polarization resistance of coatings with and without inhibitors, respectively.

3. Results and Discussion

The dispersion compositions and stabilities are summarized in Table 1. The major aspects considered during dispersion preparation were $Ce(NO_3)_3$ content and three different PTMG molecular weights. In all cases, the content of DMPA was fixed at 20 mole% [7].

First, in the polyol step, H_{12}MDI and DMPA were charged to make a NCO-terminated pre-polymer. In the second step, TEA was added to neutralize the carboxylic group. Water was added at the dispersion step. In the final step, EDA (with water) was added to the reaction mixture to complete the reaction.

In all cases, the peak at 2170 cm^{-1} disappeared (Figure 1) in the chain extension step; this confirmed the completion of the reaction [7]. The $Ce(NO_3)_3$ solution (mixed with water) was added drop-wise with vigorous stirring. The WBPU was identified by the presence of peaks at 1710 cm^{-1} and 3430 cm^{-1} for the C=O and N–H groups, respectively (Figure 1). Peaks were also recorded at 2795, 1540, and 1110 cm^{-1}. All these characteristic peaks confirmed the synthesis of PU.

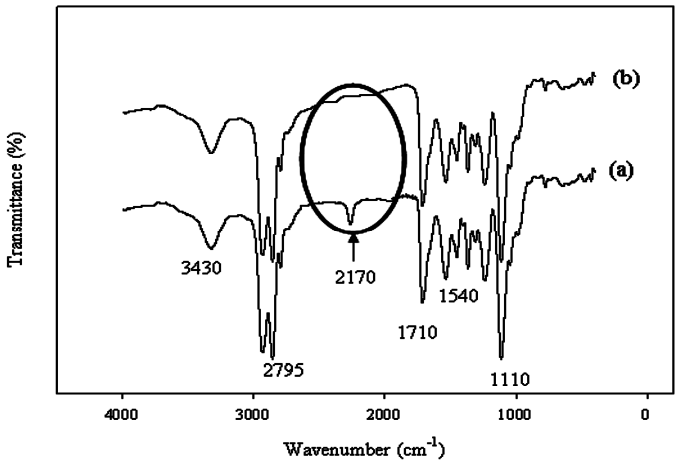

Figure 1. Fourier-transform infrared (FT-IR) spectra during polymerization (**a**) before chain extension; and (**b**) after chain extension.

The interaction between the $Ce(NO_3)_3$ and polyurethane was also studied using FT-IR analyses. Several new bands were observed (Figure 2). The bands at 1300 and 816 cm^{-1} were attributed to the NO_3^- ion vibrations. The band at 530 cm^{-1} was likely to be associated with the Ce(III) group. To evaluate the proper interaction of $Ce(NO_3)_3$ with the carboxyl acid salt group and urethane/urea group, a curve fitting technique was applied from 1530 to 1770 cm^{-1} (Figure 3). It was found that by decreasing the molecular weight of PTMG, the value at 1643 cm^{-1} for the carboxyl group shifted slightly to a higher value. This implies a strong interaction between the carboxyl acid salt and $Ce(NO_3)_3$. However, it was not possible to measure the number (one, two, or three) of carboxyl acid groups that interacted with one Ce(III) from the FT-IR analysis.

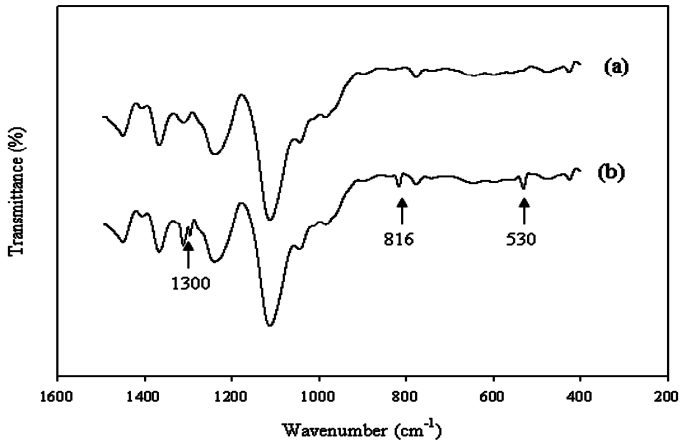

Figure 2. FT-IR spectra of WBPU during polymerization (**a**) without cerium salt; and (**b**) with cerium salt.

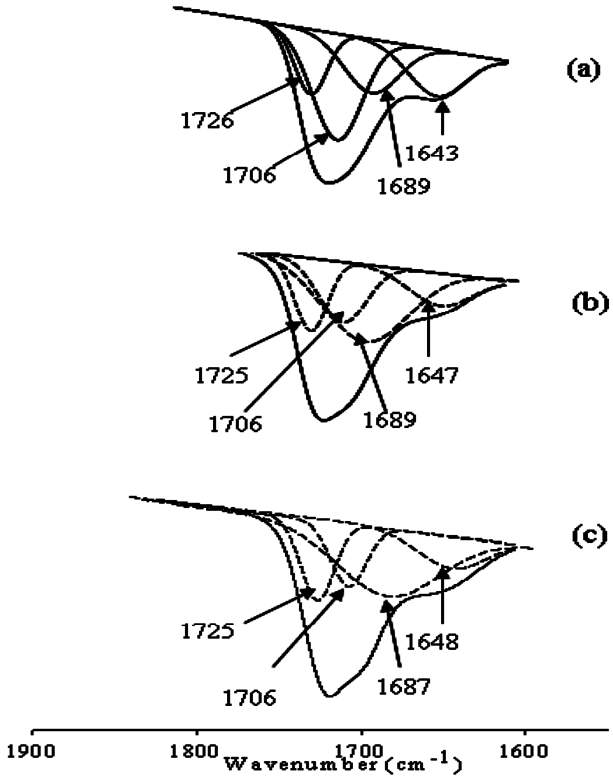

Figure 3. Curve fitting of FT-IR spectra of coatings with cerium salt of 0.008 mole from 1770 to 1530 cm^{-1}: (**a**) PTMG 2000; (**b**) PTMG 1000; and (**c**) PTMG 650.

The interaction between the carboxyl acid salt and $Ce(NO_3)_3$ was also analyzed through the XPS technique. A typical deconvoluted survey spectra using $Ce(NO_3)_3$ in the WBPU coating is shown in Figure 4. A peak at 887 eV appeared for the cerium(III) for all WBPU/$Ce(NO_3)_3$ coatings. However, with lower PTMG molecular weight (for M_n 1000 and 650), additional peaks also appeared at 888 eV for the cerium(III) of the WBPU/$Ce(NO_3)_3$ coatings. This implies that the interaction depended on the PTMG molecular weight. At higher molecular weights, the interacted carboxyl group might be one and showed one peak for cerium(III); whereas, at lower molecular weights, the interacted carboxyl group might be two or three and showed two/three peaks for cerium(III). The presence of a couple of peaks might also be due to the coordinated interaction between the cerium ion and carboxylate group. The C1s are classified into four component groups that correspond to the carbon atom of C=O (at 289.6–285.9 eV), C–C or C–H (at 282.2–285.8 eV), C–O (at 284.1–286.1 eV), and C–N (at 284.5–287.1 eV). A typical deconvoluted spectra for WBPU/$Ce(NO_3)_3$ is shown in Figure 5. Notably, the C=O is attributed to the DMPA and a broader peak from 290.7–286.0 (a higher value) with a recorded decrease of molecular weight (not shown). A broader peak usually comes from two or more peaks. This indicates that the interaction was two or three carboxyl acid salt groups. However, it was not possible to isolate these peaks from the curve analysis due to a very small broader peak. With increasing $Ce(NO_3)_3$, the intensity slightly increased for cerium(III) at respective values.

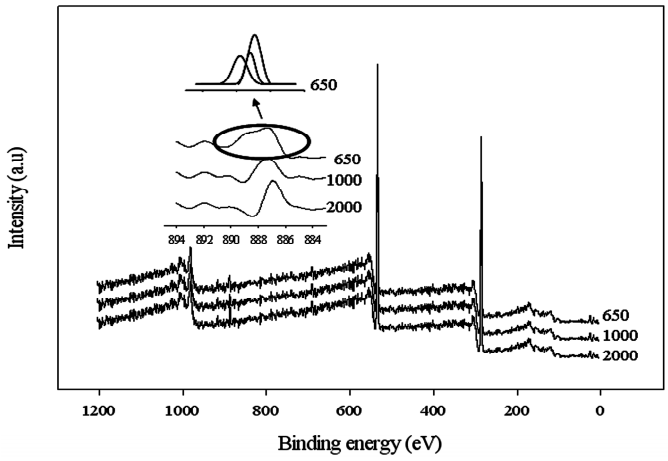

Figure 4. X-ray photoelectron spectroscopy (XPS) spectra of coatings with different molecular weight of PTMG with fixed cerium salt (0.08 mole).

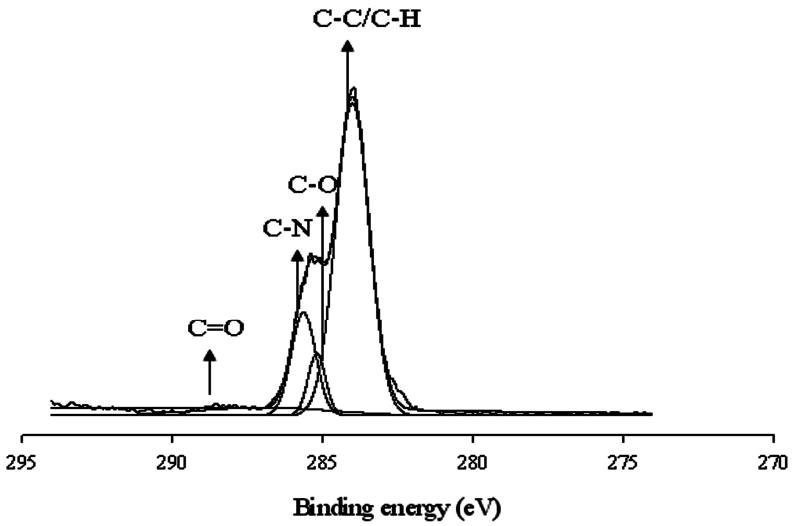

Figure 5. Deconvoluted XPS spectra of WBPU film.

All WBPU dispersions were stable with different PTMG molecular weights. The WBPU dispersion stability was affected by adding $Ce(NO_3)_3$. The dispersions were stable (no precipitation) up to a certain $Ce(NO_3)_3$ content, which also varied with the different PTMG molecular weights. The WBPU dispersions were stable up to 0.008 mole $Ce(NO_3)_3$ for all WBPU dispersions at the different PTMG molecular weights. Above 0.008 mole content, higher PTMG molecular weights yielded a higher capacity for loading $Ce(NO_3)_3$ in stable dispersions. Up to a 0.016 mole $Ce(NO_3)_3$ content could be used for a stable dispersion with PTMG 2000. This result clearly indicates that higher $Ce(NO_3)_3$ content can only be used with higher molecular weight PTMG. Researchers believe that the cerium salt (Ce^{3+}) complexes with mainly acid salts (in agreement with the FT-IR and XPS analysis), thus decreasing the free available carboxylic salt groups. As carboxyl salt is the key factor in producing a stable dispersion, increasing $Ce(NO_3)_3$ and carboxyl group complexation yielded unstable dispersions due a lack of sufficient free carboxyl salt groups. Scheme 1 shows the interaction of the cerium and carboxyl salt group complex. The precise basis for the higher cerium salt load with the higher molecular weight PTMG is unclear, and might be due to the higher content of PTMG, wherein the carboxyl groups are distal to cerium salt during complexation (see Scheme 1), which results in a lower chance of interaction of a single cerium and two or more carboxyl group complexation rate. Hence, the dispersion was stable with higher $Ce(NO_3)_3$ content and higher molecular weight PTMG. However, above 0.016 mole $Ce(NO_3)_3$, all WBPU dispersions were unstable. This might be due to the excess rate of interaction between the carboxyl acid salt and cerium.

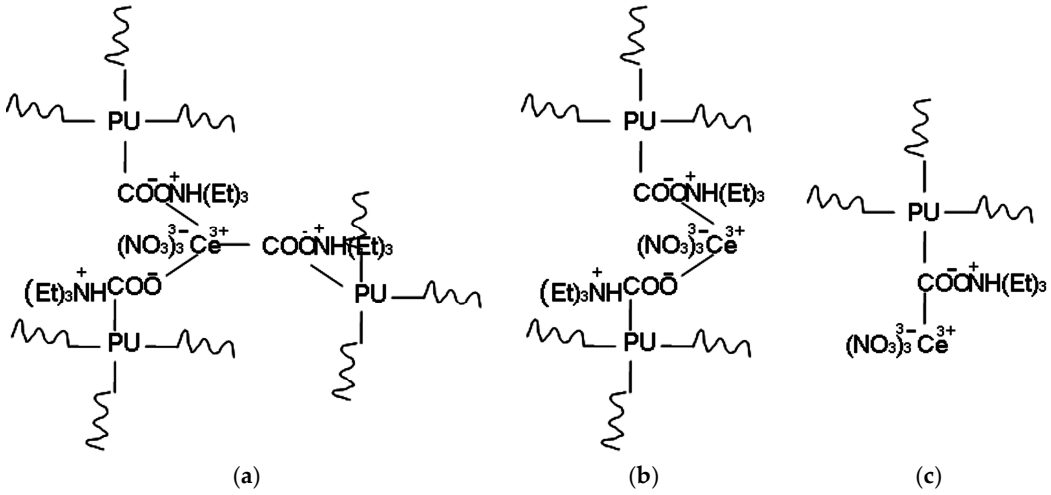

Scheme 1. Interaction of cerium salt with carboxyl acid salt: (**a**) three carboxyl acid salt; (**b**) two carboxyl acid salt; and (**c**) one carboxyl acid salt.

The dispersion stability can be described using zeta potential values. A higher magnitude of the value is an indicator of higher repulsive forces of particles, and predicts a long-term stable dispersion. If all particles in the dispersion exhibit a large negative or positive zeta potential, then they will tend to repel each other, and the particles will not tend to come together. Conversely, when the particles exhibit a lower magnitude of zeta potential, the particles come together easily to make the dispersion unstable (flocculation). Generally, the flocculation influence can be reduced or eliminated by increasing the particle charge. The zeta potential is summarized in Table 2.

Table 2. WBPU dispersions zeta potential and coatings water contact angle, water swelling, and leaching (%).

Sample	Zeta Potential (mV)	Water Contact Angle (°)	Water Swelling		Leaching (%)			
			24 h	48 h	12 h	24 h	36 h	48 h
WBPU-650	−0.49	58	17	18	–	–	–	–
WBPU-650-Ce-4	−0.38	58	20	22	50	65	71	73
WBPU-650-Ce-8	−0.22	55	23	23	63	72	77	80
WBPU-1000	−0.47	63	10	10	–	–	–	–
WBPU-1000-Ce-4	−0.42	63	10	10	35	47	52	55
WBPU-1000-Ce-8	−0.35	61	11	11	39	52	57	60
WBPU-1000-Ce-12	−0.23	58	13	13	46	59	63	69
WBPU-2000	−0.42	69	6	6	–	–	–	–
WBPU-2000-Ce-4	−0.40	68	6	6	9	19	24	30
WBPU-2000-Ce-8	−0.37	68	6	6	15	21	25	32
WBPU-2000-Ce-12	−0.35	67	7	7	17	23	28	35
WBPU-2000-Ce-16	−0.29	66	7	7	19	26	31	39

More negative values (below −40 mV) were recorded in pristine WBPU dispersions (without cerium salt). This implies a stable dispersion using different molecular weights of PTMG. However, the zeta potential value increased (less negative) by increasing the molecular weight of PTMG; this implies that the dispersion stability might have decreased with increasing PTMG molecular weight. With the addition of cerium salt, the zeta potential value changed for all dispersions. The value increased (e.g., less-stable dispersion) through an increase in $Ce(NO_3)_3$ content. However, the value changed dramatically in the low molecular weight PTMG-based dispersion. The addition of 0.004 mole cerium salt changed the zeta potential values to −11, −5, and −2 mV for WBPU-650-Ce-4, WBPU-1000-Ce-4, and WBPU-2000-Ce-4, respectively. The trend continued with increasing cerium salt content. The interaction between the carboxyl salt and cerium might be the reason why there were changes in the zeta potential value. In low molecular weight polyol, the interaction was strong due to the short chain polymer length. On the other hand, in high molecular weight polyol, the longer polymer chain might decrease the interaction due to stiff polymer chains.

Both the water contact angle and water swelling (%) tests were done to characterize the hydrophilicity of the coating. The results are summarized in Table 2. The coatings tended to swell with water at different rates. For water swelling, the WBPU films without cerium salt followed the order WBPU-2000 < WBPU-1000 < WBPU-650. As expected, the water contact angle exhibited the opposite order. These results imply that coating hydrophilicity decreased with an increase of molecular weight of PTMG. This was due to both the higher content of PTMG and the lower content of H_{12}MDI in WBPU films. The same trend was also observed using cerium salt; with fixed cerium salt, lower hydrophilicity was observed in higher PTMG molecular weight-based film. At a fixed PTMG molecular weight, the water contact angle decreased and the water swelling increased with an increase in cerium salt content. This result was prominent using higher $Ce(NO_3)_3$ content. This implies that the interaction of $Ce(NO_3)_3$ with WBPU was strong enough to change the hydrophilicity of WBPU films when a certain amount of $Ce(NO_3)_3$ was present in the film. Especially after 24 h, the water swelling increased rapidly. This confirms that $Ce(NO_3)_3$ can have a detrimental effect with longer time applications for protection.

It was found that during leaching, the coatings with different content of $Ce(NO_3)_3$ formed a porous network that facilitated the transport of inhibitors from the coating. All recorded results are summarized in Table 2. At low inhibitor loading (except the 650 series), a very slow release rate was found, which might be due to the impermeability of the coating at a certain composition. At higher $Ce(NO_3)_3$ content, large amounts of $Ce(NO_3)_3$ leach out. This promotes rapid corrosion due to a large porous structure of the coating. The leaching rate was also different with different molecular weights of PTMG at a constant $Ce(NO_3)_3$ content. The low PTMG molecular weight-based coating showed a rapid leaching compared to the high PTMG molecular weight. A high hydrophilic character of the coating using a smaller molecular weight of PTMG made water penetration comparatively very easy, which effected faster leaching. Using PTMG at a higher molecular weight, the initial leaching was very slow. However, a moderate leaching rate was recorded after 24 h.

Earlier stage coating suitability was evaluated visually. We observed no mechanical damage for all coatings. The properly dried coatings were considered for corrosion tests. The PDP is a common technique used to investigate coating anticorrosion protection. Figures 6–8 show the typical PDP curves of the 650, 1000, and 2000 series for the WBPU coatings after immersion for 1 h, respectively.

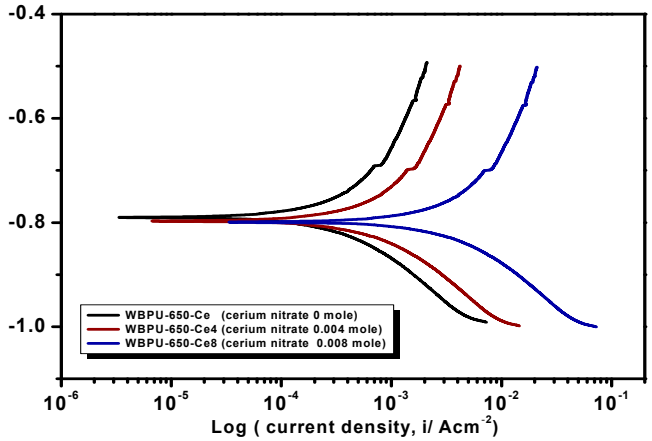

Figure 6. Potentiodynamic polarization (PDP) curves of the coatings of the PTMG 650 series with various cerium salt contents in 3.5% NaCl solution at a scan rate of 1 mV · s^{-1}.

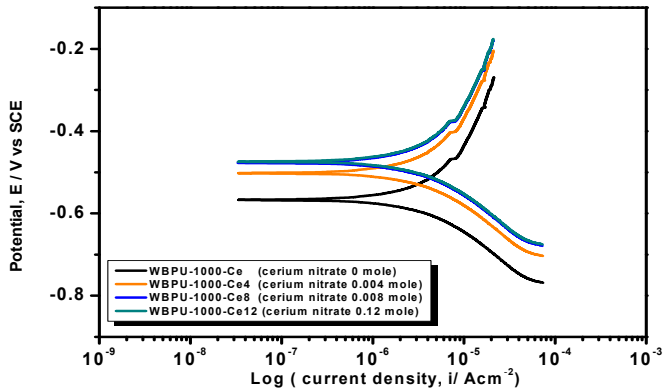

Figure 7. PDP curves of the coatings of the PTMG 1000 series with various cerium salt contents in 3.5% NaCl solution at a scan rate of 1 mV · s^{-1}.

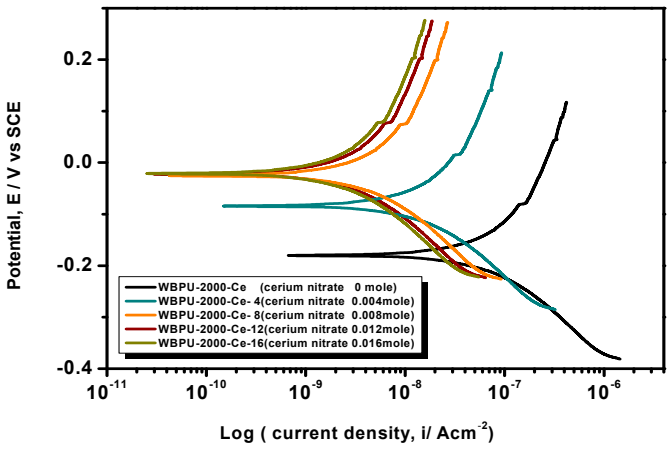

Figure 8. PDP curves of the coatings of the PTMG 2000 series with various cerium salt contents in 3.5% NaCl solution at a scan rate of 1 mV · s^{-1}.

The Tafel plot parameters are summarized in Tables 3 and 4. The E_{corr}, i_{corr}, R_p, η%, and CR all varied with respect to PTMG molecular weight and $Ce(NO_3)_3$ content. The i_{corr} value was lower in higher PTMG when compared to those for lower with similar composition ratio of WBPU dispersion. For the i_{corr} value, the WBPU films without cerium salt followed the order WBPU-650 < WBPU-1000 < WBPU-2000. In all cases, a lower value of i_{corr} was recorded with the inclusion of $Ce(NO_3)_3$ when compared to the pristine WBPU coatings, respectively. This implies that the presence of $Ce(NO_3)_3$ increased the corrosion resistance. It was also recorded that a higher $Ce(NO_3)_3$ content resulted in a lower i_{corr} value for the coating; this also implies that corrosion protection efficiency increased with higher $Ce(NO_3)_3$ content. However, up to a certain $Ce(NO_3)_3$ content, the coating exhibited a lower i_{corr} value (higher corrosion resistance) in each series; then, the i_{corr} value very slightly decreased with increasing $Ce(NO_3)_3$ content. The coating WBPU-2000-Ce-16 showed the lowest i_{corr} value among all of the coatings; this implies the highest protection for metals. As this coating provided the maximum corrosion protection, the PDP was run at different intervals of 1 h, 24 h, and 48 h (Figure 9). The i_{corr} value dropped rapidly within 48 h. Though initial corrosion protection was very good, with time, the corrosion protection decreased rapidly. This implies that the coating corrosion resistance cannot be extended by only loading higher cerium salt content. As previous leaching tests confirmed a rapid leaching of the inhibitor within 24 h, the rapid corrosion resistance decrease might therefore be due to the leaching of the inhibitor. Though earlier corrosion protection was significant using $Ce(NO_3)_3$ in the WBPU coating, a rapid leaching of cerium salt made the coating less protective for a longer time in such conditions. Therefore, this coating can be used for protecting metals from atmospheric corrosion where the chance of the inhibitor leaching is much less due to the absence of an aqueous medium. To prolong the protection in wet conditions, the leaching should be controlled as much at a low rate by improving the coating barrier properties.

Table 3. Tafel parameters of coatings with different cerium nitrate content.

Sample	E_{corr} (mV)	i_{corr} ($A \cdot cm^{-2}$)	β_a (mV/dec.)	β_c (mV/dec.)
WBPU-650	−788	3.14×10^{-3}	85	71
WBPU-650-Ce-4	−784	6.27×10^{-4}	78	69
WBPU-650-Ce-8	−774	1.66×10^{-4}	62	74
WBPU-1000	−0.565	4.21×10^{-6}	85	67
WBPU-1000-Ce-4	−0.503	3.28×10^{-6}	71	88
WBPU-1000-Ce-8	−0.480	2.63×10^{-6}	92	72
WBPU-1000-Ce-12	−0.476	2.05×10^{-6}	76	63
WBPU-2000	−0.177	1.06×10^{-7}	81	93
WBPU-2000-Ce-4	−0.072	1.69×10^{-8}	64	86
WBPU-2000-Ce-8	−0.019	4.01×10^{-9}	74	82
WBPU-2000-Ce-12	−0.016	2.96×10^{-9}	69	76
WBPU-2000-Ce-16	−0.013	2.65×10^{-9}	74	90

Table 4. Polarization resistance (R_p), inhibition efficiency (η%), and corrosion rate (CR) of coatings.

Sample	R_p ($k\Omega \cdot cm^{2)}$	η%	CR (mm/Year)
WBPU-650	5.34	–	36.404
WBPU-650-Ce-4	25.36	78.94	7.269
WBPU-650-Ce-8	88.40	93.95	1.924
WBPU-1000	4067	–	4.88×10^{-2}
WBPU-1000-Ce-4	5206	21.87	3.80×10^{-2}
WBPU-1000-Ce-8	7360	44.74	3.04×10^{-2}
WBPU-1000-Ce-12	7980	49.03	2.37×10^{-2}
WBPU-2000	18,832	–	122.89×10^{-5}
WBPU-2000-Ce-4	1,060,800	98.22	19.59×10^{-5}
WBPU-2000-Ce-8	4,334,285	99.56	4.65×10^{-5}
WBPU-2000-Ce-12	5,307,692	99.64	3.43×10^{-5}
WBPU-2000-Ce-16	6,660,000	99.71	3.07×10^{-5}

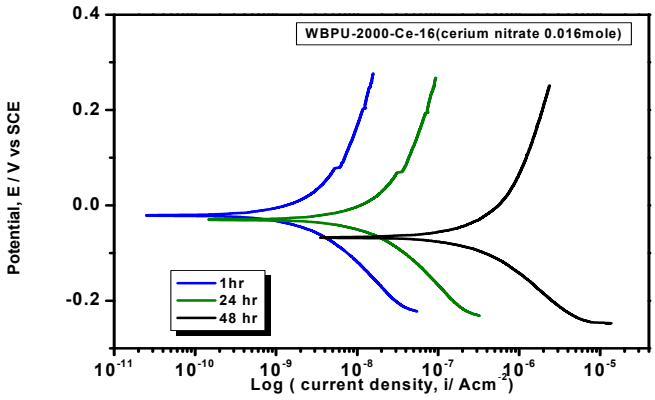

Figure 9. PDP curves of WBPU-2000-Ce-16 coating in different intervals in 3.5% NaCl solution at a scan rate of 1 mV · s^{-1}.

4. Conclusions

There is an urgent need to use fully green or less toxic materials in the coating industries. Unfortunately, most of the coatings use toxic solvents, inhibitors, and pigments. In this respect, the synthesized WBPU/$Ce(NO_3)_3$ dispersions can be considered as new green coatings. The number of interacted carboxyl groups played the key role in making the dispersion stable. The corrosion protection resistance increased with increasing $Ce(NO_3)_3$ content. The major challenge appeared in the presence of saline water, as a high release rate of cerium(III) was recorded in this condition. By improving the slow release rate of cerium(III), the protective properties of the coating can be significantly improved. Currently, this group is working on the controlled leaching of cerium(III) to improve the overall protection properties, which will be published in the near future.

Acknowledgments: This study was supported by the Center of Research Excellence in Corrosion (CoRE-C), King Fahd University of Petroleum and Minerals (KFUPM), Dhahran 31261, Saudi Arabia.

Author Contributions: Mohammad Mizanur Rahman and Md. Bashirul Haq conceived and designed the experiments; Mohammad Mizanur Rahman, Md. Hasan Zahir and Md. Bashirul Haq performed the experiments; Mohammad Mizanur Rahman, Md. Bashirul Haq, A. Madhan Kumar, and Dhafer A. Al Shehri contributed reagents/materials/analysis tools and characterization; and Mohammad Mizanur Rahman and Md. Bashirul Haq wrote the paper.

Conflicts of Interest: There is no potential conflict of interest.

References

1. Sungur, E.I.; Cotuk, A. Microbial corrosion of galvanized steel in a simulated recirculating cooling tower system. *Corros. Sci.* **2010**, *52*, 161–171. [CrossRef]
2. Syed, S. Atmospheric corrosion of carbon steel at marine sites in Saudi Arabia. *Mater. Corros.* **2010**, *61*, 238–244. [CrossRef]
3. Bat, E.; Gunduz, G.; Kisakurek, D.; Akhmedov, I.M. Synthesis and characterization of hyperbranched and air drying fatty acid based resins. *Prog. Org. Coat.* **2006**, *55*, 330–336. [CrossRef]
4. Chattopadhyay, D.K.; Raju, K.V.S.N. Structural engineering of polyurethane coatings for high performance applications. *Prog. Polym. Sci.* **2007**, *32*, 352–418. [CrossRef]
5. Chattopadhyay, D.K.; Webster, D.C. Thermal stability and flame retardancy of polyurethanes. *Prog. Polym. Sci.* **2009**, *34*, 1068–1133. [CrossRef]
6. Kim, B.S.; Kim, B.K. Enhancement of hydrolytic stability and adhesion of waterborne polyurethanes. *J. Appl. Polym. Sci.* **2005**, *97*, 1961–1969. [CrossRef]
7. Rahman, M.M.; Kim, H.D. Synthesis and characterization of waterborne polyurethane adhesives containing different amount of ionic groups (I). *J. Appl. Polym. Sci.* **2006**, *102*, 5684–5691. [CrossRef]

8. Christopher, G.; Kulandainathan, M.A.; Harichandran, G. Comparative study of effect of corrosion on mild steel with waterborne polyurethane dispersion containing graphene oxide versus carbon black nanocomposites. *Prog. Org. Coat.* **2015**, *89*, 199–211. [CrossRef]
9. Christopher, G.; Kulandainathan, M.A.; Harichandran, G. Highly dispersive waterborne polyurethane/ZnO nanocomposites for corrosion protection. *J. Coat. Technol. Res.* **2015**, *12*, 657–667. [CrossRef]
10. Coutinho, F.M.B.; Delpech, M.C. Synthesis and molecular weight determination of urethane-based anionomers. *Polym. Bull.* **1996**, *37*, 1–5. [CrossRef]
11. Coutinho, F.M.B.; Delpech, M.C.; Alves, A.S. Anionic waterborne polyurethane dispersions based on hydroxyl-terminated polybutadiene and poly(propylene glycol): Synthesis and characterization. *J. Appl. Polym. Sci.* **2001**, *80*, 566–572. [CrossRef]
12. Vakili, H.; Ramezanzadeh, B.; Amini, R. The corrosion performance and adhesion properties of the epoxy coating applied on the steel substrates treated by cerium-based conversion coatings. *Corros. Sci.* **2015**, *94*, 466–475. [CrossRef]
13. Rezaee, N.; Attar, M.M.; Ramezanzadeh, B. Studying corrosion performance, microstructure and adhesion properties of a room temperature zinc phosphate conversion coating containing $M_n{}^{2+}$ on mild steel. *Surf. Coat. Technol.* **2013**, *236*, 361–367. [CrossRef]
14. Hao, Y.; Liu, F.; Han, E.; Anjum, S.; Xu, G. The mechanism of inhibition by zinc phosphate in an epoxy coating. *Corros. Sci.* **2013**, *69*, 77–86. [CrossRef]
15. Markley, T.A.; Forsyth, M.; Hughes, A.E. Corrosion protection of AA2024-T3 using rare earth diphenyl phosphates. *Electrochim. Acta* **2007**, *52*, 4024–4031. [CrossRef]
16. Shi, H.W.; Han, E.H.; Liu, F.C. Corrosion protection of aluminium alloy 2024-T3 in 0.05 M NaCl by cerium cinnamate. *Corros. Sci.* **2011**, *53*, 2374–2384. [CrossRef]
17. White, P.A.; Hughes, A.E.; Furman, S.A.; Sherman, N.; Corrigan, P.A.; Glenn, M.A.; Lau, D.; Hardin, S.G.; Harvey, T.G.; Mardel, J.; et al. High-throughput channel arrays for inhibitor testing: Proof of concept for AA2024-T3. *Corros. Sci.* **2009**, *51*, 2279–2290. [CrossRef]
18. Yu, M.; Liu, Y.; Liu, J.; Li, S.; Xue, B.; Zhang, Y.; Yin, X. Effects of cerium salts on corrosion behaviors of Si-Zr hybrid sol-gel coatings. *Chin. J. Aeronaut.* **2015**, *28*, 600–608. [CrossRef]
19. Soestbergen, M.V.; Baukh, V.; Erich, S.J.F.; Huinink, H.P.; Adan, O.C.G. Release of cerium dibutylphosphate corrosion inhibitors from highly filled epoxy coating systems. *Prog. Org. Coat.* **2014**, *77*, 1562–1568. [CrossRef]
20. Kumar, A.M.; Rahman, M.M.; Gasem, Z.M. A promising nanocomposite from CNTs and nano-ceria: Nanostructured fillers in polyurethane coatings for surface protection. *RSC Adv.* **2015**, *5*, 63537–63544. [CrossRef]